

A study of the Influence of the Synthesis Conditions upon the Catalytic Properties of $\text{LaMnO}_{3.15}$ in Methane Combustion in the Absence and Presence of H_2S

A. Kaddouri · S. Ifrah · P. Gelin

Received: 25 February 2007 / Accepted: 17 July 2007 / Published online: 31 July 2007
© Springer Science+Business Media, LLC 2007

Abstract We report here on the activity and stability of $\text{LaMnO}_{3.15}$ for the methane combustion, in the absence and presence of H_2S , in a temperature interval of 250–750 °C. Two powders with different specific surface area were prepared by coprecipitation method using ammonia. Precursors calcined at high temperature, in air, for 10 h have led to LaMn-C solid with $S_{\text{BET}} = 11 \text{ m}^2/\text{g}$, while those previously aged in solution (hydrothermal treatment at 200 °C under 20 atm. for 24 h) then calcined at high temperature led to LaMn-HydC with $S_{\text{BET}} = 31 \text{ m}^2/\text{g}$. Temperature programmed reduction (TPR) profile of both samples showed two main peaks; surface and weakly bound oxygen named α -oxygen species and lattice oxygen β -oxygen species. While for LaMn-C the maximum reduction temperature peak corresponding to α -oxygen species was found to be *ca.* 600 °C, for LaMn-HydC samples this peak was shifted to lower temperature *ca.* 430 °C. Indeed, LaMn-HydC samples showed higher depletion of surface and weakly bound oxygen species compared to LaMn-C . The superior catalytic performance of LaMn-HydC in methane combustion was attributed to its high BET surface area and to both the high amount of

α -oxygen species and their mobility. In the presence of 100 ppm H_2S in the feed this catalyst showed a higher propensity to poisoning by sulphur compounds than LaMn-C . This was attributed to the rapid formation of stable sulphate/sulphite species, the decomposition of which occurs above 800 °C.

Keywords $\text{LaMnO}_{3.15}$ · Hydrothermal treatment · Oxygen depletion · Methane combustion · Sulphur poisoning

1 Introduction

Lanthanum based solids having the generalised perovskite structures are of considerable technological importance because of their high electronic conductivity and good chemical stability. These materials have been investigated both for use in solid oxide fuel cells (SOFC), and also as catalysts for the treatment of automobile exhaust [1–7].

Because of the ease in adjusting the composition of perovskites over a wide range, these materials can be investigated in a systematic way and correlation can be made between their performance and structure. Traditional ways of preparing perovskites materials usually adopt the mixing of oxides, hydroxides and/or carbonates constituents. However, since these compounds generally have a large particle size, this approach frequently requires repeated mixing steps and extended heating at high temperature to generate a homogeneous and single phase material.

In order to overcome the disadvantages of low surface area and limited control of the micro-structure inherent in the high temperature process, sol-gel method [8], solution combustion synthesis [9], or co-precipitation [10] of metal ions by precipitating agents have been used.

A. Kaddouri (✉) · S. Ifrah · P. Gelin
IRCELYON, Institut de recherches sur la catalyse
et l'environnement de Lyon, 2 av. Albert Einstein,
Villeurbanne, 69626, France
e-mail: akim.kaddouri@ircelyon.univ-lyon1.fr

A. Kaddouri · S. Ifrah · P. Gelin
CNRS, UMR5256, Villeurbanne, 69626, France

A. Kaddouri · S. Ifrah · P. Gelin
Université de Lyon, Lyon, 69003, France

A. Kaddouri · S. Ifrah · P. Gelin
Université Lyon 1, Lyon, 69003, France

The purpose of the present study is the synthesis of $\text{LaMnO}_{3+\delta}$ perovskites with high BET surface area using co-precipitation or a combination of co-precipitation and hydrothermal methods. Characterisation of the solids together with their catalytic activity in methane combustion in the absence and in the presence of hydrogen sulphide was also investigated.

2 Experimental

2.1 Synthesis

The catalysts $\text{LaMnO}_{3.15}$ (LaMn-C and LaMn-HydC) were prepared respectively via co-precipitation or combined co-precipitation and hydrothermal process in the presence of ammonia as precipitating agent. Reagents: $\text{La}(\text{NO}_3)_3 \cdot 6\text{H}_2\text{O}$ (98%) and $\text{Mn}(\text{NO}_3)_3 \cdot 4\text{H}_2\text{O}$ (98%), (Aldrich Chemical) were used.

Appropriate amounts of $\text{La}(\text{NO}_3)_3 \cdot 6\text{H}_2\text{O}$ and $\text{Mn}(\text{NO}_3)_3 \cdot 4\text{H}_2\text{O}$ were dissolved in distilled water, mixed and precipitated with ammonia (final pH = 8.5). On progressive ammonia addition the precipitation took place after a short time. The mixture was maintained under vigorous stirring until the obtainment of a homogeneous product which has been divided into two parts: one part was submitted to centrifugation, filtration and washing with distilled water then dried overnight at 120 °C before calcination in air at high temperature (LaMn-C sample). The second part of the sample was transferred into a Parr autoclave and submitted to a hydrothermal treatment (200 °C/20 atm./24 h) prior to calcination in a temperature interval of 600–900 °C, in air, for different periods of time (LaMn-HydC sample).

A 2%wPt/ Al_2O_3 catalysts were prepared using Al_2O_3 (SPH 569, BET: 110 m² g⁻¹) and $\text{H}_2\text{PtCl}_6 \cdot 6\text{H}_2\text{O}$ (Pt ex-Cl/ Al_2O_3) or $\text{C}_{10}\text{H}_{14}\text{O}_4$ Pt (Pt ex-acac/ Al_2O_3), and used for comparison.

2.2 Characterisation

X-ray diffractograms have been recorded with a Philips diffractometer PW 1730 using Co K α radiation ($\lambda = 1.790255$ Å) operating at 30 kV, 20 mA and scanning speed of 2° 2 Θ /min. Diffraction lines between 5 and 70° 2 Θ have been used to determine the degree of crystallinity of the calcined solids.

Thermal decomposition of LaMn-C and LaMn-HydC precursors in air was studied using a Perkin Elmer instrument Pyris Diamond TG/DTA analyser. The samples, weighing ca. 20 mg, have been placed in a platinum crucible and heated up to 850°C (with a heating rate of 10 °C/min). The gas flow rate was 60 ml min⁻¹.

SEM analyses were performed using a Hitachi 800 Microscope.

Specific surface area of the catalysts was measured at 77 K with nitrogen using a Micromeritics Tristar 3000 apparatus.

Temperature Programmed Reduction-Mass Spectrometry (TPR-MS) or Temperature Programmed Desorption-Mass Spectrometry (TPD-MS) experiments were performed from 25 up to 1150 °C (linear heating rate of 20 °C min⁻¹) using 40 mg of sample introduced in a U-shaped quartz reactor and a QMS apparatus (Pfeiffer OMNISTAR).

Catalytic runs were performed at temperatures ranging from 250 °C to 750 °C using 1% methane, 4% oxygen mixture, N₂ balance and a total flow rate of 7 L.h⁻¹. Resistance to sulphur poisoning was evaluated using 100 ppmv of H₂S in the reactant mixture. The reactor effluents were periodically sampled (each 5 min) and simultaneously analysed on line by an Agilent microchromatograph equipped with high sensitivity (5 ppm) thermal conductivity detectors.

3 Results

3.1 Catalysts Characterisation

3.1.1 Thermal Analysis of the Precursors

Thermal analysis of LaMn-C and LaMn-HydC precursors in the presence of air was investigated under similar conditions. Figure 1 presents the results of precursors decomposition profiles as a function of temperature. It is shown that the total mass loss for LaMn-C and LaMn-HydC precursors is 30.3% and 28.7%, respectively. LaMn-HydC precursor exhibits also both different decomposition rate (1%/min. vs. 0.4%/min. for LaMn-C) and mass loss with respect to LaMn-C sample, in the 640–740 °C temperature range.

3.1.2 BET Area Measurements

BET surface areas of the LaMn-C and LaMn-HydC were respectively 11 and 31 m² g⁻¹. One can note that the preparative procedure affect significantly the surface area of the catalysts. It was found that ageing for 24 h under hydrothermal conditions followed by conventional heating at 700 °C for 10 h increased drastically the surface area of $\text{LaMnO}_{3+\delta}$ perovskites.

3.1.3 X-ray Diffraction

The XRD patterns of $\text{LaMnO}_{3.15}$ (LaMn-C and LaMn-HydC) catalysts are shown in Fig. 2. Precursors aged in

Fig. 1 TG curves of lanthanum manganites precursors (LaMn-C , LaMn-HydC) decomposed in air from ambient temperature to 900°C with a heating ramp of $10^\circ\text{C min}^{-1}$

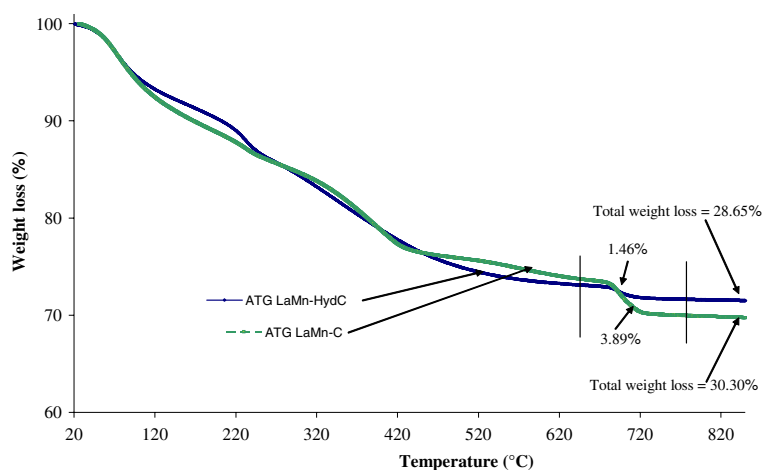
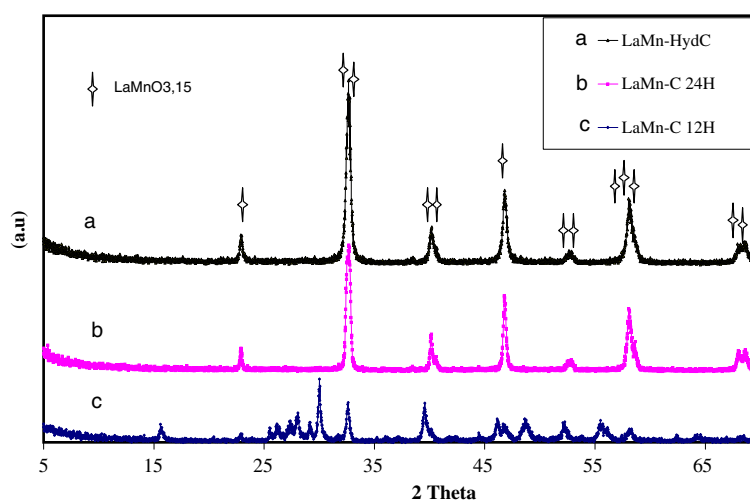


Fig. 2 X-ray diffraction patterns of lanthanum manganites precursors calcined in air at (a) $700^\circ\text{C}/10\text{ h}$ after 24 h ageing under hydrothermal conditions ($P = 20\text{ atm.}$), (b) $700^\circ\text{C}/10\text{ h}$ after 24 h ageing at atmospheric pressure (c) $700^\circ\text{C}/10\text{ h}$ after 12 h ageing at atmospheric pressure



solution, at atmospheric pressure or under hydrothermal conditions (200°C , 20 atm.) for 24 h under stirring, prior to calcination at 700°C for 10 h led to $\text{LaMnO}_{3.15}$ formation (Figs. 2a and 2b) while those aged at atmospheric pressure under stirring for only 12 h did not lead to the obtainment of the $\text{LaMnO}_{3.15}$ perovskite (Fig. 2c). The particle size calculated from the Scherrer equation was *ca.* 53 nm for LaMn-C and 26 nm for LaMn-HydC which is in agreement with BET data.

3.1.4 Temperature Programmed Reduction (TPR)

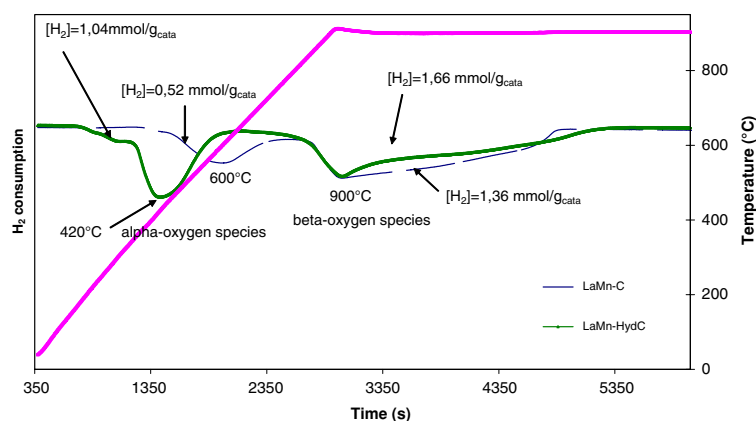
It is well known that, when a perovskite is heated at high temperature, oxygen vacancies can be formed. As thoroughly discussed in a review by Seyama [11] two types of chemisorbed oxygen species are distinguished: a low-temperature species, named α , desorbing in the $300\text{--}600^\circ\text{C}$ range, and a high-temperature one, named β , desorbing at $600\text{--}900^\circ\text{C}$.

Temperature programmed reduction (TPR) profiles of $\text{LaMnO}_{3.15}$ (LaMn-C and LaMn-HydC) catalysts are presented in Figure 3. Two main peaks appear for both samples: at *ca.* 600°C and 900°C for LaMn-C catalyst and at *ca.* 430°C and 900°C for LaMn-HydC catalyst. This suggests that there is a great mobility of α -oxygen species (first temperature reduction peak) leading to a higher reducibility of LaMn-HydC catalyst ($T_1 = 430^\circ\text{C}$, $n_1 = 1.04\text{ mmol/g}_{\text{catalyst}}$ vs. $T_2 = 600^\circ\text{C}$, $n_2 = 0.52\text{ mmol/g}_{\text{catalyst}}$ for LaMn-C). Furthermore, the total amount of oxygen species (α and β) was found to be higher in LaMn-HydC catalyst ($2.70\text{ mmol/g}_{\text{catalyst}}$ vs. $1.9\text{ mmol/g}_{\text{catalyst}}$ for LaMn-C), indicating that there is a higher amount of reducible oxygen species in this sample.

3.1.5 SEM Analyses

Figure 4 shows SEM photographs of $\text{LaMnO}_{3.15}$ (LaMn-C and LaMn-HydC) catalysts obtained after calcination at high

Fig. 3 TPR profiles of LaMn-C and LaMn-HydC catalysts



temperature. The size of LaMn-C particles (Fig. 4a) was about 0.1μ , whilst that of LaMn-HydC samples (Fig. 4b) was much smaller. Furthermore, LaMn-HydC was consisted of spherical particles while LaMn-C was more heterogeneous with different particle shapes geometries. Generally, longer synthesis times result in crystal growth, which is not the case for our experiments. Thus we may conclude that compared with the reaction time, the temperature plays a more important role in controlling the crystal morphology and size for this system.

3.2 Catalytic Activity

3.2.1 In the Absence of H_2S

Figure 5 gathers the methane conversion over perovskites catalysts as a function of temperature. It can be observed that methane conversion increases with increasing temperature for both catalysts. LaMn-C catalyst shows little activity in methane combustion below 400°C . It exhibits only 10% methane conversion at 450°C , indicating that

methane and oxygen-containing catalyst interactions were not significant at low temperature. It is noted also that T_{50} (temperature at which 50% of methane was converted into CO_2) for LaMn-HydC and LaMn-C were respectively 450°C and 550°C suggesting that LaMn-HydC is much more active for methane activation than LaMn-C catalyst. The activity of methane at 500°C was found to increase from *ca.* $0.38 \mu\text{mol/s.g}$ (LaMn-C) to *ca.* $1.18 \mu\text{mol/s.g}$ (LaMn-HydC) with the increase of BET surface area of catalysts (S_{BET} of $11 \text{ m}^2/\text{g}$ and $31 \text{ m}^2/\text{g}$, respectively).

The catalytic properties of perovskite-type oxides were compared under the same operating conditions, with that of 2%wPt/ Al_2O_3 catalysts (Fig. 5). Of the perovskites-type oxides, LaMn-HydC, exhibited a better activity than that of 2%wPt (ex-Cl)/ Al_2O_3 in the temperature range of $250\text{--}550^\circ\text{C}$. For temperatures lower than 550°C , 2%wPt (ex-acac)/ Al_2O_3 functioned as the best catalyst of those examined in the present study, whilst LaMn-C had appeared to be the poorest catalyst for methane combustion. Suppression of activity increase was more stressed for perovskite LaMn-C at elevated temperatures while both

Fig. 4 SEM photographs of (a) LaMn-C and (b) LaMn-HydC catalysts

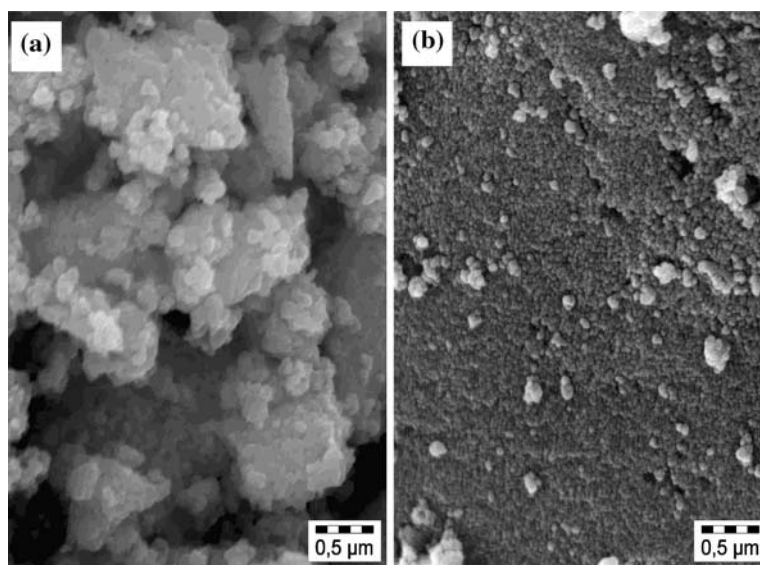
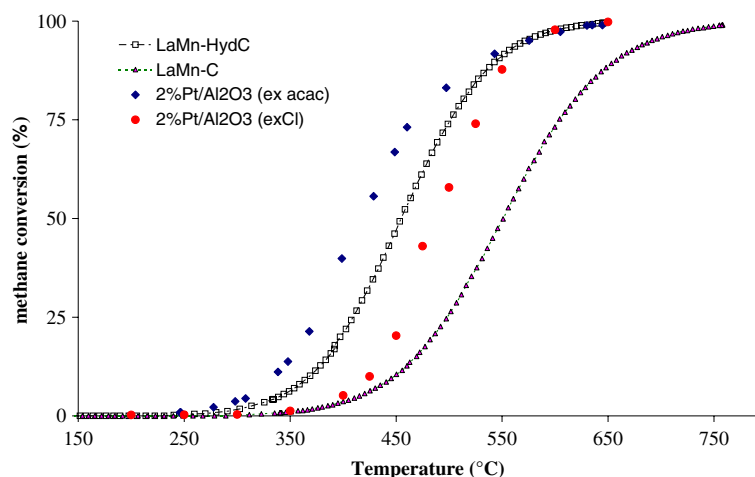


Fig. 5 % CH_4 conversion vs. temperature over LaMn-C , LaMn-HydC , 2%wPt (ex-Cl)/ Al_2O_3 and 2%wPt (ex-acac)/ Al_2O_3 catalysts in methane combustion



2%wPt/ Al_2O_3 and LaMn-HydC catalysts showed similar level of activity at $T > 550$ °C [12].

3.3 Catalytic Tests in the Presence of H_2S

The presence of H_2S (100 ppmv) in the feed caused a decrease in the activity of both perovskites (Fig. 6). However, LaMn-C catalyst was found to be more resistant to sulphur poisoning than LaMn-HydC catalyst. For a better assessment of the sensitivity to sulphur poisoning of perovskites and for comparison with metal supported catalysts, a sample of 2%wPt (ex-acac)/ Al_2O_3 was also exposed 30 h to 100 ppmv H_2S . As seen in Fig. 6, 2%wPt (ex-acac)/ Al_2O_3 lost its activity significantly faster than LaMn-HydC and LaMn-C . After *ca.* 4 h testing it retained about 35.3 % of its original activity versus 70.3% and 83.1% for LaMn-HydC and LaMn-C , respectively. Initial deactivation rates were 51.4, 5.3 and 2.95 $\mu\text{mol/s.g}$ for 2%wPt (ex-acac)/ Al_2O_3 , LaMn-HydC and LaMn-C , respectively. The effect of exposure for progressively longer times on-stream on the catalytic activity showed that 2%wPt (ex-acac)/ Al_2O_3 undergo a negligible deactivation between 4 and 30 h testing. On the contrary, the deactivation was slow but evident for LaMn-C and drastic for LaMn-HydC . After *ca.* 30 h testing the activity of 2%wPt (ex-acac)/ Al_2O_3 and LaMn-C catalysts was nearly identical, while LaMn-HydC deactivated completely. No structural modifications of the samples were observed by XRD.

3.3.1 TPD after H_2S Treatment

TPD profiles of both sulphur poisoned $\text{LaMnO}_{3.15}$ catalysts (LaMn-C and LaMn-HydC) were presented in Figs. 7 and 8 respectively. Two main peaks appeared in both catalysts: at

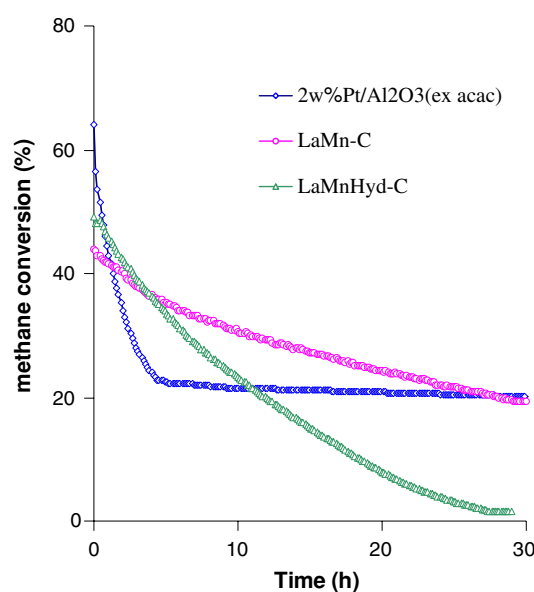


Fig. 6 Effect of H_2S on the catalytic activity of LaMn-C , LaMn-HydC and 2%wPt (ex-acac)/ Al_2O_3 in methane combustion

866 °C and 994 °C for LaMn-C and at 830 °C and 930 °C for LaMn-HydC . These peaks were attributed to sulphate/sulphite species decomposition leading to SO_2/O_2 release. The total amount of SO_2 desorbed from LaMn-C and from LaMn-HydC samples were respectively 1.0×10^{-3} and *ca.* 0.7×10^{-3} $\text{mol/g}_{\text{catalyst}}$. Furthermore, the temperature of maximum oxygen depletion (peak at *ca.* 660 °C) for LaMn-HydC was highly shifted after sulphur poisoning towards higher temperatures ($T \geq 750$ °C). The same phenomenon was observed for LaMn-C excepted that the peak at *ca.* 627 °C, characteristic of α -oxygen species observed in the fresh sample, split into two peaks respectively at 667 °C and 772 °C. The presence of the lower temperature peak (667 °C) reflects that the activity of LaMn-C towards methane changed upon exposure of H_2S but is not strongly

inhibited. Therefore, it can be derived that oxygen mobility in H_2S poisoned LaMn-C and LaMn-HydC catalysts is affected differently, which is in agreement with the different rates of catalytic activity decrease with time (Fig. 6).

4 Discussion

$\text{LaMnO}_{3.15}$ catalysts were prepared, using co-precipitation method, and aged either at atmospheric pressure or under hydrothermal conditions then calcined at high temperatures. The hydrothermal method which was investigated in this study seemed to be promising for producing homogeneous powders consisting of stoichiometric particles with spherical morphologies and sizes of less than 100 nm. The hydrothermal ageing of the precursors in the synthesis process, was shown as an efficient method preventing the particle aggregation during the calcination process, as demonstrated by both BET and SEM.

In the case of samples aged at atmospheric pressure, it has been clearly observed that the catalyst particles, resulting from LaMn-C precursor calcination at 700 °C for 10 h, have highly irregular shapes, larger particles size while still having the perovskite crystal structure.

Thus the degree of reaction of manganese with lanthanum ions at the synthesis temperature and pressure affects significantly the way in which perovskite particles grow after nucleation. The changes of BET surface area, morphology, amounts and mobility of oxygen species of both solids prepared (at atmospheric pressure or under hydrothermal conditions) will have a significant effect on catalytic activity.

Methane oxidation activity of $\text{LaMnO}_{3.15}$ perovskites with different surface areas depicted in the form of light-off temperature (LOT) curves (Fig. 5) indicates a gradual decrease in the LOT (temperature of reaction initiation) of methane oxidation (increase in activity) with an increase in

the surface area of the perovskites [13]. A shift in the light-off temperature for a given reaction has been generally found to depend on the method of preparation and sintering [14, 15].

Moreover, the results of TPR investigations reported in Fig. 3 showed that the active α -oxygen species increased with the increase of BET surface area of catalysts while the temperature of β -oxygen species depletion remained constant (900 °C). The presence of hydrogen seems to anticipate respectively by *ca.* 27 °C and 230 °C, the loss of α -oxygen species compared to TPD experiments.

The close parallel between catalytic activity for methane combustion, in the absence of H_2S , and the extent of α -oxygen species indicates that the combustion over LaMn-C and LaMn-HydC perovskites is much better with LaMn-HydC and it would proceed mainly through a supra-facial catalytic mechanism [16].

As far as the effects of catalysts exposure to hydrogen sulphide on the catalytic activity are concerned, Fig. 6 clearly shows that LaMn-C and LaMn-HydC catalysts have different behaviours. LaMn-C catalyst showed better stability in the presence of hydrogen sulphide. After 30 h exposure to 100 ppmv H_2S it still conserve *ca.* 50% of its initial activity. The catalytic properties of perovskite-type oxides were compared with those of 2%wPt (ex-acac)/ Al_2O_3 (Fig. 6). It was observed that, after 30 h exposure to 100 ppmv H_2S , the resistance to sulphur poisoning of LaMn-C and 2%wPt (ex-acac)/ Al_2O_3 was comparable. On the contrary, the sensitivity to sulphur poisoning of LaMn-HydC was important and the catalyst deactivated completely. The poisoning of metal oxide catalysts by sulphur compounds can be due to the presence of preferential adsorption sites for SO_2 molecules. Depending on the surface morphology of the catalysts, sulphur oxide may adsorb in a variety of forms [17]. Some of the highly active oxygen species present in LaMn-HydC catalyst may lead to a rapid formation of sulphates blocking the active sites.

Fig. 7 TPD profile of sulphur-poisoned LaMn-C catalyst

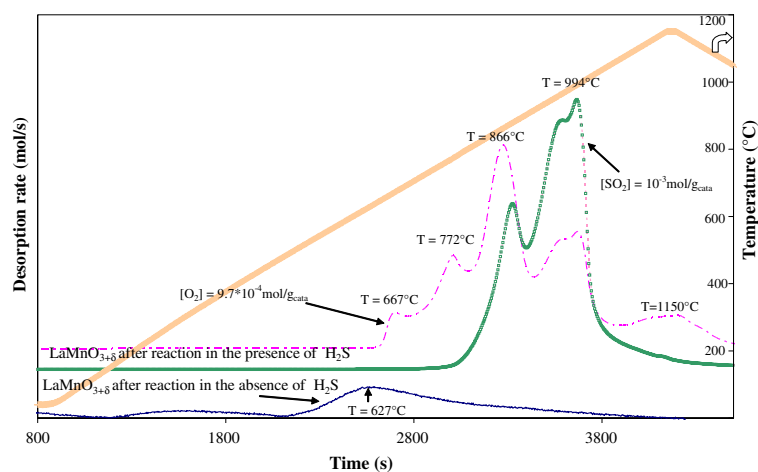
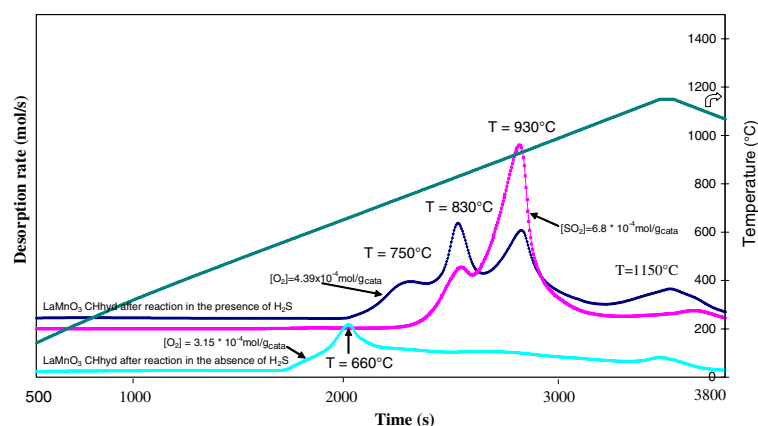


Fig. 8 TPD profile of sulphur-poisoned LaMn-HydC catalyst

Sulphates/sulphites formation takes place on both the LaMn-C and LaMn-HydC catalysts. TPD experiments performed with LaMn-HydC showed the presence of much less amounts of sulphates/sulphites species than over LaMn-C catalysts. However, the peaks characteristic of desorption of sulphates/sulphite species from LaMn-C surface were shifted to higher temperatures with respect to those observed with LaMn-HydC catalysts. Therefore, the different behaviour of LaMn-C and LaMn-HydC catalysts towards sulphur poisoning could be thought due to the structural differences of the catalysts at atomic scale.

Finally, it is clear that the hydrothermal synthesis of this dual cations perovskite oxide produce, after thermal treatment at 700 °C for 10 h, fine $\text{LaMnO}_{3.15}$ powder (LaMn-HydC) with both good stoichiometry and high BET surface area. However, despite these advantages, this material is sensitive to sulphur poisoning when exposed 30 h to 100 ppm H_2S . Overcoming such difficulty, however, hydrothermal synthesis would give significant benefits not only for preparation of this material but would also give useful insights concerning the synthesis of many similar multi-cations perovskite materials.

Although perovskite catalysts investigated in this study are far from optimal and cannot be proposed as potential automotive catalysts due to the high concentrations of sulphur present in combustion products of automotive fuels, they may find applications in other situations, for example in catalytic natural gas combustion, where the levels of sulphur compounds are rather low.

Previous studies [18, 19] on the effect of SO_2 on MgO -doped lanthanum manganese or on MgO -doped lanthanum-chromium-manganese oxides activity showed that MgO , up to a certain amount, played a protecting role against sulphur poisoning. Magnesium oxide was considered to be a possible preferential site for SO_2 molecules. Catalytic methane combustion over MgO -doped LaMn-HydC catalysts in the presence of sulphur containing compounds is in progress.

5 Conclusion

$\text{LaMnO}_{3.15}$ catalysts with uniform morphologies and controllable size have been synthesised by co-precipitation method, in presence of ammonia, and ageing under hydrothermal conditions. The hydrothermal treatment was used to regulate the nucleation and particle growth in the following step of calcination of the precursors, so the final BET surface area and size of catalyst particles can be well controlled. The TPR profiles of catalysts showed the ability of LaMn-HydC to provide α oxygen species at low (430 °C) temperature (vs. 600 °C for LaMn-C), suggesting a great mobility of weakly bound and surface oxygen species in this catalyst. The superior catalytic activity of LaMn-HydC with respect to that of LaMn-C was attributed to both the higher reducibility and to the greater amount of reducible α -oxygen species.

Both LaMn-C and LaMn-HydC perovskites were found to deactivate in the presence of 100 ppm H_2S in the feed showing their different propensity to poisoning by sulphur compounds. This was attributed to the rapid formation of stable sulphate/sulphite species, the decomposition of which occurs above 800 °C.

References

1. Banzal NP, Zhong Z (2006) *J Power Sour* 158:148
2. Monterrubio-Badillo C, Ageorges H, Chartier T, Coudert JF, Fauchais P (2006) *Surf Coat Technol* 200:3743
3. Vashook V, Vasylechko L, Zosel J, Muller R, Ahlborn E, Guth U (2004) *Solid State Ionics* 175:151
4. Simner SP, Shelton JP, Anderson MD, Stevenson JW (2003) *Solid State Ionics* 161:11
5. Labhsetwar NK, Watanabe A, Biniwale RB, Kumar R, Mitsuhashi T (2001) *Appl Catal B: Environ* 33:165
6. Fino D, Russo N, Cauda E, Saracco G, Specchia V (2006) *Catal Today* 114:31
7. Zhang-Steenwinkel Y, Van der Zande LM, Castricum HL, Blik A, Van den Brink RW, Elzinga GD (2005) *Chem Eng Sci* 60:797
8. Barnabe A, Gaudon M, Bernard C, Laberty C, Durand B (2004) *Mater Res Bull* 39:725

9. Fumo DA, Mirelli MR, Segadaes AM (1996) *Mater Res Bull* 31:1255
10. Guillemet-Fritsch S, Alphonse P, Calmet C, Coradin H, Tailhades P, Rousset A (2005) *Compt Rend Chim* 8:219
11. Seyama T (1992) *Catal Rev Sci Eng* 34:281
12. Arai H, Hamada T, Eguchi K, Seyama T (1986) *Appl Catal* 26:265
13. Gunasekaran N, Saddawi S, Carberry JJ (1996) *J Catal* 159:107
14. Kirchnerova J, Klvana D, Vaillancourt J, Chaouki J (1993) *Catal Lett* 21:77
15. Barnard KR, Fogar K, Turney TW, Williams RD (1990) *J Catal* 125:265
16. Voorhoeve RJH, Remeika JP, Trimble LE (1976) *Ann NY Acad Sci* 2:272
17. Kung HH (1989) *Studies in Surface Science and Catalysis*, vol. 45. Elsevier, New York, p. 169
18. Rosso I, Saracco G, Specchia V, Garrone E (2003) *Appl Catal B: Environ.* 40(3):195
19. Rosso I, Garrone E, Geobaldo F, Onoda B, Saracco G, Specchia V (2001) *Appl Catal B: Environ* 34(1):29